General Disclaimer

One or more of the Following Statements may affect this Document

- This document has been reproduced from the best copy furnished by the organizational source. It is being released in the interest of making available as much information as possible.

- This document may contain data, which exceeds the sheet parameters. It was furnished in this condition by the organizational source and is the best copy available.

- This document may contain tone-on-tone or color graphs, charts and/or pictures, which have been reproduced in black and white.

- This document is paginated as submitted by the original source.

- Portions of this document are not fully legible due to the historical nature of some of the material. However, it is the best reproduction available from the original submission.

NASA

Technical Memorandum 86065

The Influence of Ground Conductivity on the Structure of RF Radiation from Return Strokes

D. M. LeVine and L. Gesell

FEBRUARY 1984

THE INFLUENCE OF GROUND CONDUCTIVITY ON THE STRUCTURE

OF RF RADIATION FROM RETURN STROKES

D. M. LeVine
Goddard Laboratory for Atmospheric Sciences
Goddard Space Flight Center
Greenbelt, MD   20771

L. Gesell
System Engineering and Development Corporation
Columbia, MD   21045

February 1984

GODDARD SPACE FLIGHT CENTER
Greenbelt, Maryland 20771

THE INFLUENCE OF GROUND CONDUCTIVITY ON THE STRUCTURE OF RF RADIATION FROM RETURN STROKES

D. M. LeVine
Goddard Laboratory for Atmospheric Sciences
Goddard Space Flight Center
Greenbelt, MD   20771

L. Gesell
System Engineering and Development Corporation
Columbia, MD   21045

ABSTRACT

Simultaneous measurements of fast electric field changes and RF radiation from first return strokes indicate that a time delay exists between the first noticeable RF radiation and the beginning of the return stroke as determined from the fast field change. Measurements in Florida showed this delay to be on the order of 20 μs in the HF–UHF range. Similar results have been found by this author in experiments in New Mexico (TRIP-79) and in Virginia at NASA's Wallops Flight Facility.

It will be shown in this paper that the combination of the finite conductivity of the earth plus the propagation of the return stroke current up the channel results in an apparent time delay between the fast field changes and RF radiation for distant observers. The time delay predicted from model return strokes is on the order of 20 μs and the received signal has the characteristics of the data observed in Virginia and Florida.

The theoretical work has been done using a piecewise–linear model for the return stroke channel and a "transmission line" model for current propagation on each segment.

iii

Radiation from each segment is calculated over a flat earth with finite conductivity using asymptotic approximations for the Sommerfeld integrals. The radiation at the observer is then "processed" by a model AM radio receiver. The output voltage has been calculated for several frequencies between HF-UHF assuming a system bandwidth (300 kHz) characteristic of the system used to collect data in Florida and Virginia. Comparison with the theoretical fast field changes indicates a time delay of the order of 20 μs.

THE INFLUENCE OF GROUND CONDUCTIVITY ON THE STRUCTURE OF RF RADIATION FROM RETURN STROKES

I. INTRODUCTION

When measurements are made of RF radiation from the first return strokes of cloud-to-ground lightning flashes it is observed that the RF radiation does not start with the beginning of the return stroke as indicated by its fast electric field change but rather begins several 10's of microseconds later. This time delay was first reported by Brook and Kitagawa (1964) and Takagi (1969a, b) in measurements made in New Mexico, and later was investigated by Le Vine and Krider (1977) in measurements made during the Thunderstorm International Research Project (TRIP) in Florida. Le Vine and Krider (1977) reported a relatively constant delay of about 20 μs at several frequencies between 3 MHz and 300 MHz. The existence of such a time delay is particularly surprising in return strokes because the electric field changes from first return strokes are known to begin quite abruptly (Weidman and Krider, 1978; Lin et al., 1979; Tiller, et al., 1976; Guo and Krider, 1982); consequently one would expect the beginning of the return stroke to be associated with radiation over a large range of frequencies, including RF. It is the purpose of this paper to show that this intuition is correct but that when the effects of the dispersive conductivity of the earth on the radiation from the return strokes is taken into account the effect is an apparent time delay.

In the sections to follow, a review will be given first of the measurements establishing the existence of the time delay. Examples will be presented from data collected by Le Vine and Krider in Florida and by Le Vine at Langmuir Laboratory in New Mexico and at NASA's Wallops Flight Facility in Virginia. Then theory will be presented for radiation from return strokes in which the effects of a finitely conducting earth are included. The theoretical work employs a piecewise linear model for the return stroke channel and a "transmission line" model for the current on each segment.

This model is used to calculate the electric field radiated from the return stroke over a conducting earth using an asymptotic approximation which is valid for observers far from the channel. The electric field is assumed to be the input to an ideal AM radio receiver similar to those used in the experiments and a mathematical model for the receiver is used to calculate the receiver output voltage at several frequencies. Comparison of these calculations with the beginning of the return stroke indicates a time delay consistent with experiment.

II. THE TIME DELAY

Figure 1 is a block diagram of an experiment of the type used by Le Vine and Krider (1977) and also by Le Vine (this paper) to observe the time delay. In these experiments measurements were made of the radiation from first return strokes of lightning flashes using a fast electric field change system (Uman, 1969; Krider et al., 1977) and also an AM radio receiver. The two signals v ere recorded simultaneously and stored on a digital sample and hold device (e.g., a Biomation model 8100 waveform recorder) to obtain high time resolution. The analogue output of the waveform recorder was displayed on a dual beam oscilloscope and photographed for a permanent record. Experiments of this sort have been performed by Le Vine and Krider in Florida (Le Vine and Krider. 1977) and by Le Vine at Langmuir Laboratory in New Mexico during TRIP-79 and at NASA's Wallops Flight Facility in Virginia during the summers of 1979 and 1980 as part of NASA's Storm Hazards program (Pitts, 1982). The instrumentation used in all of these experiments was similar to that used by Le Vine and Krider (1977) in Florida. The RF receivers used at frequencies greater than 30 MHz were commercially available AM receivers (Watkins-Johnson models WJ-977 and WJ-8730 with WJ-9082 tuning heads) and at frequencies of 3 MHz and 30 MHz they were fixed tuned receivers specially designed by the Georgia Institute of Technology (Le Vine et al., 1976). The output of each receiver was filtered to provide a signal with a common bandwidth (300 kHz) at all frequencies. In the measurements in Florida, dipoles were used at all frequencies, but in the later measurements the dipoles were replaced with disk cone antennas at frequencies greater than 50 MHz. The fast field change system was designed by Krider (Krider, et al., 1977) and consisted of a flat plate antenna about 30 cm in diameter followed by an integrator. The integrator compensates for the capacitive impedance of the electrically small antenna so that the output voltage is proportional to the incident electric field, E(t). The time constant of the integrator was about 1 ms, which determined the low frequency response of the system (about 1 kHz) and the high frequency response (several MHz) was determined by the operational amplifier used in the integrator. It is in this frequency range that most of the energy radiated from return strokes is to be found (Oh, 1969:

3

Le Vine, 1980; Kimpara, 1965; Horner, 1964; Cianos, Oetzel and Pierce, 1972). Consequently, the fast field change system provides a measure of the overall shape of the waveform radiated from return strokes. The high frequency detail it lacks is the information provided by the radio receivers.

Figures 2 and 3 are examples of lightning data collected in Florida with this system. The lower trace in each figure is the fast field change from a first return stroke and the upper trace is RF radiation at 295 MHz. These examples are part of the data set collected by Le Vine and Krider during TRIP-76 (Le Vine and Krider, 1977) but not previously published. The fast field change consists of a sequence of small pulses preceding an abrupt jump in the electric field (center). The large field change in the center of the record is characteristic of fast electric field changes associated with first return strokes (Weidman and Krider, 1978; Tiller et al., 1976; Lin et al., 1979) and the preceding sequence of pulses are typical of radiation from the stepped leaders which proceed the return stroke (Krider et al., 1977). The top trace in each figure is the voltage output of a radio receiver tuned to 295 MHz. (Figure 3 is an example of horizontally polarized radiation. All other examples in this paper are for vertically polarized radiation.) Clearly, there is detectible radiation at this frequency during the return stroke. However, the radiation does not begin with the abrupt transition in the incident E(t) as one would expect; rather, it begins 10 or 20 μs after the initiation of the fast field change and does not reach a maximum (the horizontal lines indicate receiver saturation) for several 10's of μs after the beginning of the return stroke. A similar delay between the beginning of the fast electric field change and the beginning of the RF radiation was observed at all frequencies (3-300 MHz) at which measurements were made in Florida (Le Vine and Krider, 1977). Similar results have also been obtained by Le Vine in measurements at NASA's Wallops Flight Facility in Virginia and at Langmuir Laboratory in New Mexico. Figures 4 and 5 are examples of vertically polarized radiation collected at 3 MHz (Figure 4) and at 139 MHz (Figure 5) in Virginia and Figures 6 and 7 are examples of the fast electric field change and RF radiation at 3 MHz and 170 MHz, respectively, collected during TRIP-79 at Langmuir Laboratory in New Mexico. The time delays observed in

4

these experiments were on the order of 20 μs except in Virginia where the delay at 139 MHz was closer to 40 μs. A consistent feature of the data is the rather abrupt beginning of the RF radiation at the higher frequencies (e.g., Figures 2, 3, and 5) but the gradual increase in signal level at 3 MHz (e.g., Figure 4; Le Vine and Krider, 1977, Figure 2).

III. RECEIVER RESPONSE TO RADIATION FROM RETURN STROKES

It is the objective of the remainder of this paper to show that a time delay in the RF radiation from return strokes is a natural consequence of the dispersive dielectric constant of the earth and the propagation of the return stroke current up the lightning channel. This will be done theoretically by adopting a model for the return stroke, using this model to compute the radiated electric field, and then processing this radiation through a model RF receiver similar to those used in the experiments.

The standard AM radio receivers used during the experiments are devices which amplify and detect the envelope of an amplitude modulated sinusoid. In practice this is normally done by translating the input signal to an intermediate frequency where the actual detection is done. However, the net effect is simply that of an envelope detector in series with a filter which represents the effective bandwidth and gain of the system. It can be shown (Appendix A) that the voltage, $V_0(t)$, out of such a system tuned to a frequency, ν_0, is

$$V_0(t) = \left| \int_{-\infty}^{\infty} a(\nu_0 + \zeta)E_z(\nu_0 + \zeta)H(\zeta)e^{-j2\pi\zeta t}d\zeta \right| \tag{1}$$

where the bars $|\ |$ indicate the magnitude of the complex number inside, $E_z(\nu)$ is the spectrum (Fourier transform) of the vertical component of the electric field radiated to the receiver from the return stroke, $a(\nu)$ represents the effect of the antenna and system gain, and where $H(\nu)$ is a filter representing the equivalent bandwidth of the system. Equation 1 is obtained under the assumption that the bandwidth of the system is small compared to the nominal frequency, ν_0, to which the receiver is tuned.

In order to compute the receiver output voltage, $V_0(t)$, the spectrum $E_z(\nu)$ of the incident radiation is required. This will be computed here by adopting a piecewise-linear version of what is commonly called a "transmission line" model for return strokes. The first step in this procedure is to create a channel out of linear segments placed end-to-end in a computer generated random walk.

6

The procedure is suggestive of the manner in which channels are formed in real lightning by the stepped leader. In the implementation of this procedure, a probability distribution is chosen for the change in cartesian coordinates that occur in going from the beginning of one segment to its other end. The coordinates themselves are selected by the computer "at random" from this distribution. Details and examples are given by Le Vine and Meneghini (1978a). A change in this procedure adopted by Le Vine since 1978 has been to use two probability distributions. The second distribution is used to vary the statistics (the mean) of the first distribution. This gives a channel with small scale fluctuations (tortuosity) determined by the primary distribution and these are superimposed on large scale randomly changing drifts determined by the second distribution. Figure 8 is an example of a channel generated in this manner. The second distribution determines the rather long (several hundred meter) drift of the channel to the left or right. The two scale model was adopted after statistical comparison of computer generated channels with photographs of lightning channels. The two scale model not only yielded the most realistic looking channels, but it was also necessary to get the correlation between junction points to agree with the data (photographs). A two scale channel model was also found to be necessary by Ribner and Roy (1981) to achieve satisfactory simulation of thunder.

Given the channel, the return stroke is modelled by a current pulse which propagates along each segment with constant velocity. That is, it is assumed that the current on each segment has the form $I(t - \hat{\ell}_i \cdot \bar{r}_i / v_i)$ where $\hat{\ell}_i$ is a unit vector along the i-th segment in the direction of current flow and v_i is the velocity of propagation of the current pulse along the i-th segment. In the literature on lightning, this model for the current is called a "transmission line" model. It was originally suggested by Dennis and Pierce (1964) and developed formally by Uman and colleagues (Uman et al., 1973; Uman and McLain, 1969; McLain and Uman, 1971) who also demonstrated agreement with data (Uman et al., 1973). The variation employed here is a piecewise-linear adaption of the model which permits the effects of channel tortuosity to be included (Le Vine and Meneghini, 1978a; Le Vine, 1980; Le Vine and Meneghini, 1983).

7

The fundamental analytic problem in this model is to calculate the electromagnetic fields radiated from each segment. Given the solution the computer can be programmed to obtain the total field at a particular observation point by summing the contribution from each segment, keeping track of the phase as the current pulse propagates up the channel. This will be done here for an observation point near the ground and far from the channel compared to the channel length. A solution will be obtained for each element which takes into account the conductivity of the earth.

The effect of the conductivity of the earth is included in the calculations by using Norton's form for the solution for radiation from a dipole above a conducting earth (Norton, 1937). In the case of an observer very far from the element compared to the height of the element above the surface asymptotic approximations result in a particularly simple form (Appendix B) and the solution for the vertical (i.e., z–component) of electric field at the surface can be written:

$$E_z(\nu) = \Delta_h E_{hz}^{\infty}(\nu) + \Delta_v E_{vz}^{\infty}(\nu) \tag{2}$$

where $E_{hz}^{\infty}(\nu)$ and $E_{vz}^{\infty}(\nu)$ are the solutions for the z–components of electric field due to a filament above a perfectly conducting ($\sigma = \infty$) ground plane oriented parallel (E_{hz}^{∞}) or perpendicular (E_{vz}^{∞}) to the surface. The $\Delta_{h,v}$ are correction factors which account for the finite conductivity of the ground:

$$\Delta_v = \frac{\zeta}{1 + \zeta} \tag{3a}$$

$$\Delta_h = \frac{\zeta}{1 + \zeta} \left[1 + j \frac{R}{k (z')^2 (1 + \zeta)} \right] \tag{3b}$$

where $\zeta = (z'/R)\sqrt{\epsilon_r}$ and ϵ_r is the (complex) relative dielectric constant of the earth ($\epsilon_r = \epsilon_r' + j\, \epsilon_r''$), z' is the height of the element above the surface, R is the distance from the element to the observer and $k = 2\pi\nu/c$.

8

The $E_{hz}^{\infty}(\nu)$ and $E_{vz}^{\infty}(\nu)$ in Equation 2 are the solutions for radiation from a straight segment above a perfectly conducting plane driven by the propagating current pulse $I(t - \hat{\ell}_i \cdot \vec{r}_i / v_i)$. In the frequency domain this current is $I(\nu)e^{jk\eta\hat{\ell}_i \cdot \vec{r}_i}$ where $\eta_i = c/v_i$. The solution is similar to that from a linear travelling wave antenna and can be obtained using a fraunhofer approximation (e.g., Le Vine and Meneghini, 1978a, b). One obtains

$$E_{(h,v),z}^{\infty}(\nu) = \sqrt{(\mu/\epsilon)}\, I(\nu)\, \frac{\epsilon_{h,v}}{2\pi R}\, [e^{jk\tau+} - e^{jk\tau-}] \qquad (4)$$

where

$$\tau\pm = \frac{R}{c} \pm \frac{L}{2c}(\eta + \hat{\ell} \cdot \nabla R) + \tau_0 \qquad (5a)$$

$$\epsilon_v = \frac{(\hat{\ell} \cdot \hat{z}) - (\hat{\ell} \cdot \hat{z})(\hat{z} \cdot \nabla R)^2}{\eta - (\hat{\ell} \cdot \nabla R)} \qquad (5b)$$

$$\epsilon_h = -\frac{(\hat{\ell} \cdot \nabla R)(\hat{z} \cdot \nabla R) - (\hat{\ell} \cdot \hat{z})(\hat{z} \cdot \nabla R)^2}{\eta - (\hat{\ell} \cdot \nabla R)} \qquad (5c)$$

In this expression L is the length of the segment and τ_0 is a constant needed to keep track of the phase of the current pulse as it propagates from element to element. The two terms in the solution corresponding to $\tau\pm$ mathematically appears as if they come from the ends of the filament (e.g., see Le Vine and Meneghini, 1978a, b): The terms $\pm\frac{L}{2c}(\hat{\ell} \cdot \nabla R)$ are the linear terms in a binomial expansion of the time for propagation from each of the ends of the filament to the observer and $L\eta/2c$ accounts for the time (L/v) required for the pulse to propagate from one end of the filament to the other. The total electric field at the observation point is the sum over all elements. Using Equations 2 and 4 it can be written in the form:

$$E_z(\nu) = \frac{\sqrt{\mu/\epsilon}}{2\pi}\, I(\nu) \sum_{\text{all } i} \frac{1}{R_i} [\Delta_{h_i} \epsilon_{h_i} + \Delta_{v_i} \epsilon_{v_i}]\, [e^{jk\tau_i+} - e^{jk\tau_i-}] \qquad (6)$$

The voltage output of the radio receiver can now be computed by substituting Equation 6 into Equation 1. One obtains:

$$V_o(t) = \left| \frac{\sqrt{\mu/\epsilon}}{2\pi} a(\nu_o) I(\nu_o) \int_{-\infty}^{\infty} \sum_{\text{all } i} \frac{1}{R_i} [\Delta_{h_i}(\nu_o)\epsilon_{h_i} + \Delta_{v}(\nu_o)\epsilon_{v_i}] \cdot \right.$$

$$\left. \cdot [e^{j2\pi(\nu_o + \zeta)\tau_i^+} - e^{j2\pi(\nu_o + \xi)\tau_i^-}] H(\xi)e^{-j2\pi\xi t} d\xi \right| \qquad (7)$$

where it has been assumed that over the passband of the filter $H(\zeta)$, the factors $a(\nu)$, $I(\nu)$ and the $\Delta_{h,v}(\nu)$ are essentially constant. This is a good approximation for receivers such as those used by Le Vine (Le Vine et al., 1976) and Le Vine and Krider (1977) to measure time delay which had an effective bandwidth of about 300 kHz and made measurements at 3 MHz or more. (At 3 MHz the bandwidth is 10% and at 300 MHz the bandwidth is only 0.1%.) Recognizing that the integral in Equation 7 is a Fourier transform, one obtains:

$$V_o(t) = \left| \frac{\sqrt{\mu/\epsilon}}{2\pi} a(\nu_o) I(\nu_o) \sum_{\text{all } i} \frac{1}{R_i} [\Delta_{h_i}(\nu_o)\epsilon_{h_i} + \Delta_{v_i}(\nu_o)\epsilon_{v_i}] \cdot \right.$$

$$\left. \cdot [h(t-\tau_i^+)e^{j2\pi\nu_o\tau_i^+} - h(t-\tau_i^-)e^{j2\pi\nu_o\tau_i^-}] \right| \qquad (8)$$

where $h(t)$ is the temporal, complex analytic, response of the filter (e.g., Born and Wolf, 1959).

IV. RESULTS

Calculations have been made of the receiver output, $V_o(t)$, for several different frequencies ν_o using Equation 8 and letting the observer be on the x-axis 100 km from the base of the channel. The calculations were performed by first constructing a return stroke channel using linear segments placed end-to-end as described above. The change in cartesian coordinates of the end points were selected from a normal distribution with standard deviations $\sigma_x = \sigma_y = 3.8$ m and $\sigma_z = 6.0$ m and means $m_x = m_y = 0.05$ m and $m_z = 8.0$ m. The means of the x and y components were changed at randomly selected intervals using numbers from another normal distribution with zero mean and $\sigma_x = \sigma_y = 0.58$ m. These numbers were chosen to give agreement with statistics on the tortuosity of lightning channels obtained from photographs of lightning. The compound exponential model $I(t) = I_0(e^{-\alpha t} - e^{-\beta t}) + I_1(e^{-\gamma t} - e^{-\delta t})$ was chosen for the current. The current pulse is based on a form proposed by Uman (1969) and others (e.g., Uman and McLain, 1969). The first two exponentials represent the main pulse in a form proposed by Bruce and Golde (1941) and the second pair of exponentials represent ..termediate current (Uman, 1969). The parameter values used were $\alpha = 4 \times 10^4$ sec^{-1}, $\beta = 8 \times 10^5$ sec^{-1}, $\gamma = 10^3$ sec^{-1}, $\delta = 2 \times 10^4$ sec^{-1}, $I_0 = 30$ kA and $I_1 = 2.5$ kA which were based on the values suggested by Dennis and Pierce (1964) but modified slightly to reflect recent evidence that the rise time of the current pulse should be more rapid (e.g., Clifford, Krider, and Uman, 1979; Weidman and Krider, 1980). The velocity of propagation of the current pulse up the channel was chosen to be 10^8 m/s which is representative of return strokes (Uman, 1969) and for convenience it was constant on all segments. The system filter was chosen to be $h(t) = (1/T) \sin^2(t\pi/2T)$ $0 < t < T$ and zero otherwise. The form for $h(t)$ was chosen largely for convenience of computation. It's passband in the frequency domain is approximately $1/T$ wide which was chosen to be about 330 kHz ($T = 3 \times 10^{-6}$ seconds) and the scale factor $1/T$ multiplying the sinusoid is used so that the filter has approximately unit gain over its passband. Finally, the factor $a(\nu)$ which includes the detector gain and the effect of the antenna was chosen arbitrarily to be unity.

Figures 9 and 10 are examples of $V_0(t)$ at 3 MHz (Figure 9) and at 130 MHz (Figure 10) from the channel shown in Figure 8. The lower trace in each figure is $V_0(t)$ for a channel over a perfectly conducting ground ($\sigma = \infty$) and the upper example was obtained using the dielectric constant of soil given by Hoekstra and Delaney (1974; Figure 13). The time axes on these figures have been adjusted so that zero corresponds to the time when radiation from the beginning of the return stroke would first reach the observer. Notice that in the case of a perfectly conducting ground plane, the radiation begins abruptly at very nearly the time radiation is expected from the beginning of the return stroke. A small delay is present because the system is causal and is essentially determined by the impulse response, $h(t)$, of the filter. In contrast, when realistic values of ϵ_r are used for the ground plane (top curves in Figures 9 and 10) the receiver output shows a gradual increase, building from a small value at the beginning of the return stroke to a function of time which eventually looks like that from a return stroke over a perfectly conducting ground plane. (Notice that the amplitude of $V_0(t)$ as plotted in Figures 9 and 10 has been normalized by $I(\nu)$ the spectrum of the current pulse at the frequency, ν_0. The normalization factors are given in the figure captions. Using the normalization factors one finds that the signal level at 3 MHz is about 1.9×10^3 greater than at 130 MHz because $I(\nu)$ is very much smaller at 130 MHz than at 3 MHz. The same normalization has been used, independent of ϵ_r. Hence from Figure 9 one sees that radiation at 3 MHz from a return stroke above a perfectly conducting ground earth is about 5 times as great as from the same channel over a more realistic soil.)

A convenient interpretation of the results shown in Figures 9 and 10 can be obtained by noticing that $\tau_i{}^+ = \tau_{i+1}^-$ in Equation 8. This is true because the top of one segment coincides with the bottom of the adjoining segment. Using this result, Equation 8 can be written

$$V_0(t) = \left| \frac{\sqrt{\mu/\epsilon}}{2\pi} \, a(\nu_0) I(\nu_0) \sum_{\text{all } i} \frac{(a_i - a_{i+1})}{R_i} \, h(t - \tau_i{}^+) e^{j2\pi\nu_0\tau_i^+} \right| \qquad (9a)$$

where

12

$$a_i = \Delta_{h_i}(\nu_o)\epsilon_{h_i} + \Delta_{v_i}(\nu_o)\epsilon_{v_i} \qquad (9b)$$

In this form. it is clear that the radiation detected by the receiver appears to come from the junctions between segments (Le Vine and Meneghini, 1978a, b) and that the receiver response to the radiation from such a junction is its impulse response, h(t), weighted by the factor $(a_i - a_{i+1})/R_i$. This amplitude depends on the relative orientation of the segments, being large when the angle between segments is large and small for segments which are nearly parallel ($a_i = a_{i+1}$). All junctions do not radiate simultaneously because the current pulse is propagating up the channel with finite velocity. Consequently. the sum in Equation 8 is only over those junctions which the current pulse has reached. Furthermore, h(t) has a finite width (i.e., is nonzero only in the interval $t - T < t < t + T$) and this further limits the junctions contributing to $V_o(t)$ to those which have been illuminated within ±T seconds of t. Hence, one can imagine a window 2vT meters long moving up the channel at the velocity v of the propagation of the current pulse. The signal $V_o(t)$ out of the receiver comes from junctions which lie within this window. At the instant radiation begins (i.e.. current starts up the channel) the receiver detects radiation from a single junction (the base of the channel) and the receiver output has the shape h(t). the receiver impulse response. As the current pulse advances up the channel radiation comes from an increasing number of junctions and the receiver output increases correspondingly. Eventually, a steady state is reached in which a new junction is added to the filter window $t - T < t < t + T$ by the advancing current pulse as old ones leave. The amplitude of $V_o(t)$ in this "steady state" is determined by the values of $a_i - a_{i+1}$. Finally, when the current pulse reaches the top of the channel, the amplitude decreases as radiation from fewer and fewer junctions is passed by the filter. This occurs at about 65 μs in Figures 9 and 10.

When the surface is a perfectly conducting boundary $\Delta_h = \Delta_v = 1$ and only the relative orientation of adjoining segments affect the receiver output. In fact, a careful examination of Figures 7-9 shows that the peaks in $V_o(t)$ when $\sigma = \infty$ correspond to elements that join at large angles.

13

When the boundary is not a perfect conductor, the interpretation of the receiver response as described above is still appropriate, but now the amplitude of the radiation is modified by the $\Delta_{h,v}$. For frequencies above a few MHz and observers far from the channel (i.e., $R \gg z'$), one finds that $\Delta_h \cong \Delta_v = \zeta/(1 + \zeta)$ where $\zeta = z'\sqrt{\epsilon_r}/R$. Consequently, one expects $V_0(t)$ to have the same general structure as in the perfectly conducting case but with its amplitude decreased by $\Delta_v(\nu)$. $\Delta_v(\nu)$ is a function of the height of the radiating junction above the surface, and Figure 11 is a plot of $\Delta_v(\nu)$ as a function of height for several different frequencies. These curves were obtained using the values given by Hoekstra and Delaney (1974; Figure 13) for the dielectric constant of soil. One sees from Figure 11 that radiation from junctions close to the surface is severely attenuated and that this attenuation decreases with increasing height above the surface. At frequencies less than a few 100 kHz the attenuation is significant only very near the surface, whereas at frequencies of 1 MHz or more the attenuation is significant even at the top of a lightning channel. Because the current in return strokes propagates up the channel, height can be associated with time, the time it takes the current to reach a particular altitude. This time has been indicated on Figure 11 using $v = 10^8$ m/s for the velocity of propagation of the current pulse. For example, consider an observer at $R = 50$ km from the channel. Then the current pulse reaches 5 km ($x = 0.1$) in 50 μs ($T = 1.0$).

The effect on $V_0(t)$ of this change in $\Delta_v(\nu)$ with time is clearly evident in the upper examples in Figures 9 and 10. In each case $V_0(t)$ exhibits a gradual increase with time which is determined by the increase in $\Delta_v(\nu)$ that takes place as the current pulse propagates up the channel. Comparison with the radiation when the channel is over a perfectly conducting ground plane (bottom of each figure) shows that $V_0(t)$ has the same structure (i.e., same peaks and valleys) in both cases, as is especially evident at the ends of the record (e.g., near $t = 50$ μs), but with an amplitude which initially increases with time. This is so because the structure is determined by the shape of the channel which is the same in both cases and $\Delta(\nu)$ is changing from a constant value of unity for the perfectly conducting ground plane to a value which increases with height in the case of a realistic soil.

14

Another set of examples is shown in Figure 12 for a different lightning channel. The channel in this case is shown on the left and at the top right are $V_0(t)$ for receivers tuned to 3 MHz and 130 MHz and at the bottom are the receiver responses at these frequencies in the case of a perfectly conducting ground plane. The attenuation of the radiation emanating from the lower portions of the channel when the conductivity of the ground is taken into account is clearly evident in these examples.

Finally, Figure 13 shows the average receiver response obtained from three different channels all generated from the same statistical distribution. The attenuation of radiation coming from near the base of the channel is clearly evident when comparison is made with radiation from the same channel over a perfectly conducting ground plane (bottom).

V. CONCLUSION

This paper has attempted to show that the time delay observed between arrival of fast electric field changes and RF radiation from first return strokes can be explained in terms of conventional models for return strokes by including the effect of the conductivity of the ground. This was done using a piecewise linear adaptation of the transmission line model for return strokes and using a solution patterned after that by Norton (1937) to account for the effect of the conductivity of the ground on the electric field radiated to a distant observer. The radiated electric field was then used as the input to a model AM radio receiver to calculate the RF radiation at different frequencies from the return stroke. It was shown that the radiation from different portions of the return stroke is attenuated compared to the radiation from an identical channel over a perfectly conducting ground plane. This attenuation is height dependent, being larger for portions of the return stroke near the base of the channel and decreasing for portions of the channel further from the surface. When this attenuation is combined with the fact that the return stroke current propagates up the channel at finite velocity, the result is a time dependent attenuation of the receiver output voltage. It was shown that the receiver output voltage is initially small because of severe attenuation of the RF radiation from elements of the channel near the ground and then the signal increases as the radiating elements are located further and further from the ground. This means that the receiver will not detect radiation from the return stroke until the current has propagated sufficiently high above the ground that radiation from this portion of the channel exceeds the detection threshold. If the conductivity of the earth were constant as a function of frequency, a similar delay would be expected in the output from a conventional fast field change system. However, the conductivity of the earth is very strongly a function of frequency below a few MHz and the imaginary part of the relative dielectric constant of slightly moist soil is on the order of 10^5 at 1 kHz and 10^3 at 100 kHz. Consequently, at the frequencies which determine the gross shape of fast electric field changes it seems reasonable to assume that radiation takes place over a perfectly conducting ground plane. Thus, the fast field changes arrive at the observer with its shape largely unaffected by the ground

16

plane (of course the rise time and other high frequency detail will be affected) whereas the RF radiation, especially at VHF and above, will have been attenuated during the initial portions of the return stroke. The result is an apparent difference in the time of arrival at the observer between the beginning of the return stroke as deduced from the fast field change and the detection of the RF radiation.

REFERENCES

Baños, A., Dipole Radiation in the Presence of a Conducting Half-Plane, Pergamon Press, New York 1966.

Born, M., and E. Wolf, Principles of Optics, Pergamon Press, 1959.

Brook, M., and N. Kitagawa, "Radiation from Lightning Discharges in the Frequency Range 400-1000 Mc/s," J. Geophys. Res., 69, 2431-2434, 1964.

Bruce, C. E. R., and R. H. Golde, "The Lightning Discharge," J. Inst. Elec. Eng., London, 88, (No. 11), pp. 487-505, 1941.

Cianos, N., G. N. Oetzel and E. T. Pierce, "Structure of Lightning Noise — Especially Above HF," Lightning and Static Electricity Conference, Wright Patterson AFB, December 1972.

Clifford, D., E. P. Krider and M. Uman, "A Case for Submicrosecond Rise-Time Lightning Current Pulses for Use in Aircraft Induced Coupling Studies," Proc. International Conference on Electromagnetic Compatibility, pp. 143-149, 1979.

Dennis, A. S., and E. T. Pierce, "The Return Stroke of the Lightning Flash to Earth as a Source of VLF Atmospherics," Radio Science, 68D (No. 7), pp. 777-794, 1964.

Guo, C., and E. P. Krider, "The Optical and Radiation Field Signatures Produced by Lightning Return Strokes," J. Geophys. Res., 87. pp. 8913-8922, 1982.

Hoekstra, P., and A. Delaney, "Dielectric Properties of Soils at VHF and Microwave Frequencies," J. Geophys. Res., 79 (No. 11), pp. 1699-1702, 1974.

Horner, F., "Radio Noise from Thunderstorms," in Advances in Radio Research, Vol. 2, Academic Press, J. A. Saxton, ed., pp. 122-204, 1964.

Jones, D. S., The Theory of Electromagnetism, Pergamon Press, New York, 1964.

Kimpara, A., "Electromagnetic Energy Radiated from Lightning," in Problems in Atmospheric and Space Electricity, S. C. Coroniti, ed., Elsevier Pub. Co., pp. 352–365, 1965.

Kraus, J. D., Radio Astronomy, McGraw-Hill Book Co., 1966.

Krider, E. P., C. D. Weidman, and R. C. Noggle, "The Electric Fields Produced by Lightning Stepped Leaders." J. Geophys. Res., 82, pp. 951–960, 1977.

Le Vine, D. M., "The Spectrum of Radiation from Lightning," Proc. IEEE International Symposium on Electromagnetic Compatibility, pp. 249–253, October, 1980.

Le Vine, D. M. and E. P. Krider, "The Temporal Structure of HF and VHF Radiations During Florida Lightning Return Strokes." Geophys. Res. Lett., 4, pp. 13–16, 1977.

Le Vine, D. M. and R. Meneghini, "A Solution for the Electromagnetic Fields Close to a Lightning Discharge," Proc. International Conference on Lightning and Static Electricity, Fort Worth, Texas, pp. 70-1 to 70-10, June, 1983.

Le Vine, D. M. and R. Meneghini, "Simulation of Radiation from Lightning Return Strokes: The Effects of Tortuosity," Radio Science, 13, p. 801, 1978a.

Le Vine, D. M., and R. Meneghini, "Electromagnetic Fields Radiated from a Lightning Return Stroke: Application of an Exact Solution to Maxwell's Equations," J. Geophys. Res., 83, pp. 2377–2384, 1978b.

Le Vine, D. M., et al., The Structure of Lightning Flashes HF-UHF: September 12, 1975, Atlanta, Georgia, NASA X-953-76-176, 1976.

Lin, Y. T., M. A. Uman, J. A. Tiller, R. D. Brantley, W. H. Beasley, E. P. Krider, and C. D. Weidman. "Characterization of Lightning Return Stroke Electric and Magnetic Fields from Simultaneous Two-Station Measurements." J. Geophys. Res., 84 (C10), pp. 6307–6314, 1979.

Lin, Y. T., M. A. Uman and R. A. Standler, "Lightning Return Stroke Models, J. Geophys. Res., 83 (C 9), pp. 1571-1583, 1980.

McLain, D. K., and M. A. Uman, "Exact Expression and Moment Approximation for the Electric Field Intensity of the Lightning Return Stroke," J. Geophys. Res., 76 (No. 9), pp. 2101–2105, 1971.

Norton, K. A., "The Propagation of Radio Waves Over the Surface of the Earth and the Upper Atmosphere," Proc. IRE, 25 (No. 9), pp. 1203-1237, 1937.

Oh, L. L., "Measured and Calculated Spectral Amplitude Distribution of Lightning Sferics," IEEE Trans., EMC-11 (4), pp. 125-130, 1969.

Pitts, F. L., "Electromagnetic Measurements of Lightning Strikes to Aircraft," AIAA J. of Aircraft. 19, pp. 246-250, 1982.

Ribner, H. S., and D. Roy, "Thunder from Tortuous Lightning: A Computer Model Made Audible," Proc. AIAA 7th Aeroacoustics Conference, Palo Alto, California, October 5-7, 1981.

Sommerfeld, A. N., Annals of Physics, pp. 113, 1926.

Stratton, J. A., Electromagnetic Theory, McGraw-Hill, 1941.

Takagi, M., "VHF Radiation from Ground Discharges," in Planetary Electrodynamics, Proceedings of the 4th International Conference on the Universal Aspects of Atmospheric Electricity, edited by S. C. Coroniti and J. Hughes, Gordon and Breach, New York, pp. 535-538, 1969a.

Takagi, M., "VHF Radiation from Ground Discharges," in Proc. Res. Inst. Atmospherics, Nagoya Univ., Japan, pp. 163-168, 1969b.

Tiller, J. A., M. A. Uman, Y. T. Lin, R. D. Brantley and E. P. Krider, "Electric Field Statistics for Close Lightning Return Strokes near Gainsville, Florida," J. Geophys. Res., 81, pp. 4430-4434, 1976.

Uman, M. A., Lightning, McGraw-Hill, 1969.

Uman, M. A., D. K. McLain, R. J. Fisher and E. P. Krider, "Electric Field Intensity of the Lightning Return Stroke," J. Geophys. Res., 78 (No. 18), pp. 3523-3529, 1973.

Uman, M. A. and D. K. McLain, "Magnetic Field of Lightning Return Stroke," J. Geophys. Res., 74 (No. 28), pp. 6899-6910, 1969.

Wait, J. R., "The Electromagnetic Fields of a Horizontal Dipole in the Presence of a Conducting Half-Space," Can. J. Phys., 3, pp. 1017-1028, 1961.

Weidman, C. D. and E. P. Krider, "The Fine Structure of Lightning Return Strokes Waveforms," J. Geophys. Res., 83, pp. 6239-6247, 1978.

Weidman and C. D. and E. P. Krider, "Submicrosecond Rise Times in Lightning Return Stroke Fields," Geophys. Res. Lettrs., 7, pp. 955-958, 1980.
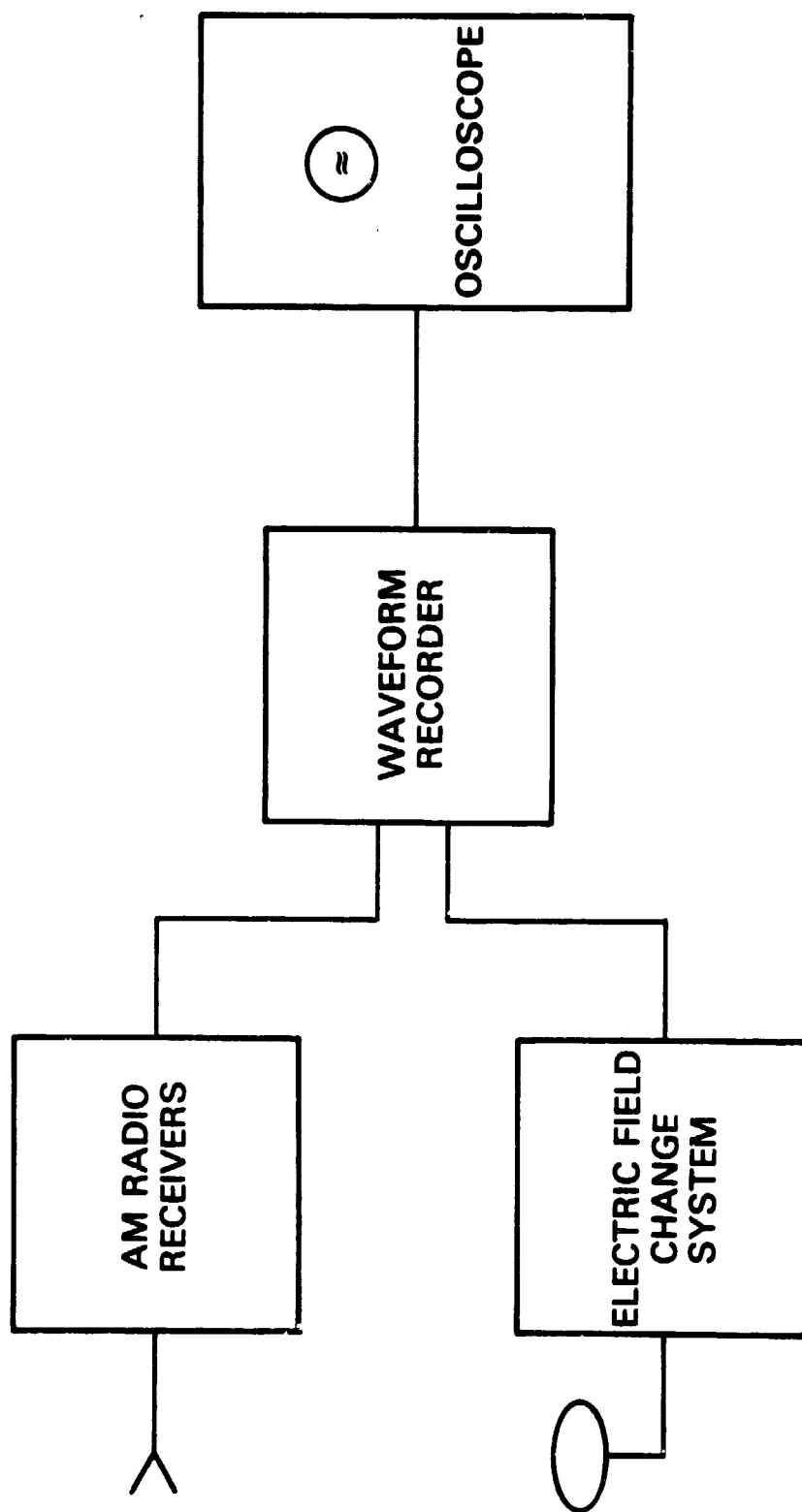
Figure 1. Schematic of experiment to measure time delay.

23
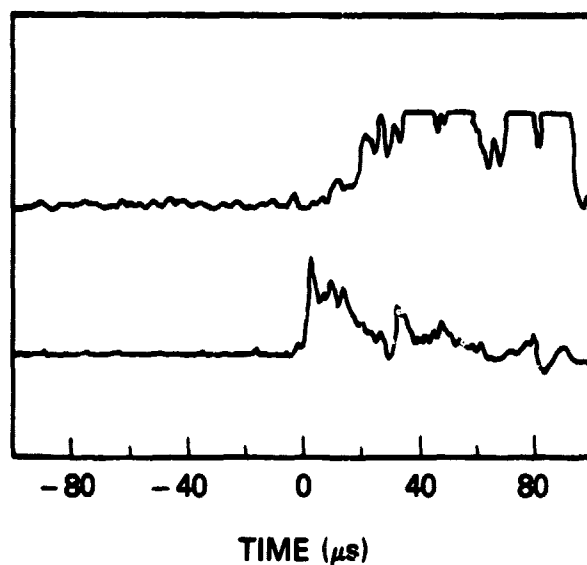
Figure 2. Fast electric field change (bottom) and vertically
polarized radiation at 295 MHz (top) from lightning in
Florida at the Kennedy Space Center. The data was recorded
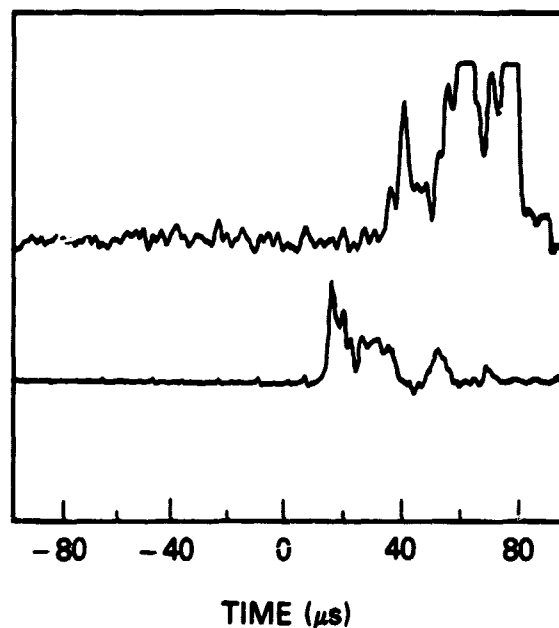during TRIP-76 on July 16, 1976.

Figure 3. Fast electric field change (bottom) and horizontally
polarized radiation at 295 MHz from lightning (top) recorded
at the Kennedy Space Center, Florida. The data were recorded
during TRIP-76 on July 10, 1976.

TIME (μs)
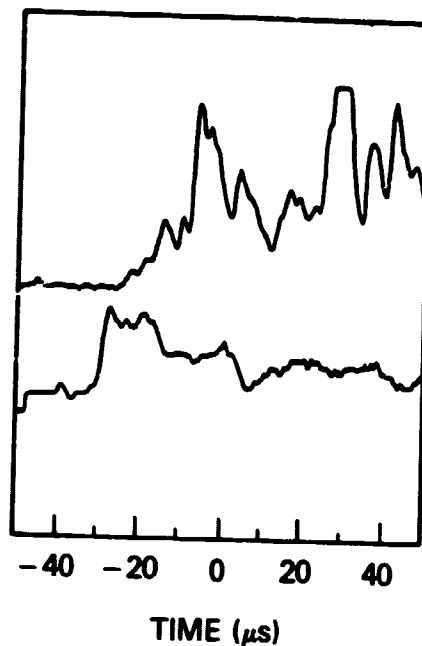
Figure 4. Fast electric field change (bottom) and vertically
polarized radiation at 3 MHz from lightning in Virginia. The
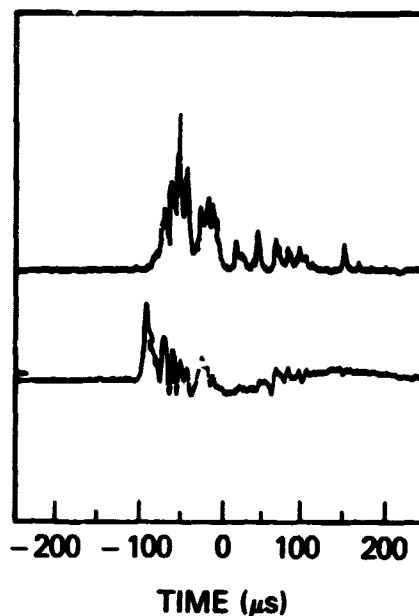data were recorded on July 29, 1979 at the Wallops Flight
Facility, Virginia.

TIME (μs)
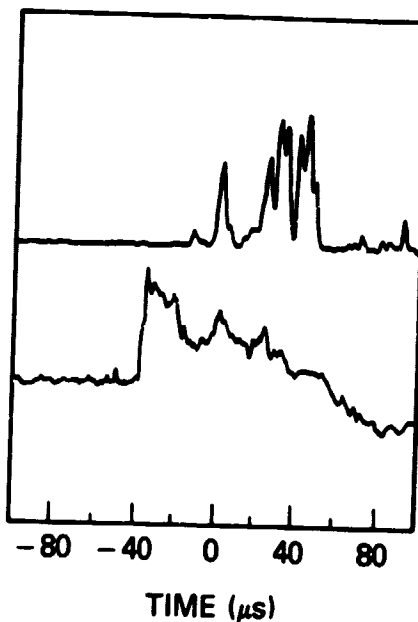
Figure 5. Fast electric field change (bottom) and vertically
polarized radiation at 139 MHz from lightning in Virginia. The
data were recorded on July 29, 1979 at the Wallops Flight
Facility, Virginia.

25

Figure 6. Fast electric field change (bottom) and vertically
polarized radiation at 3 MHz (top) from lightning in New
Mexico. The data were recorded near Langmuir Laboratory
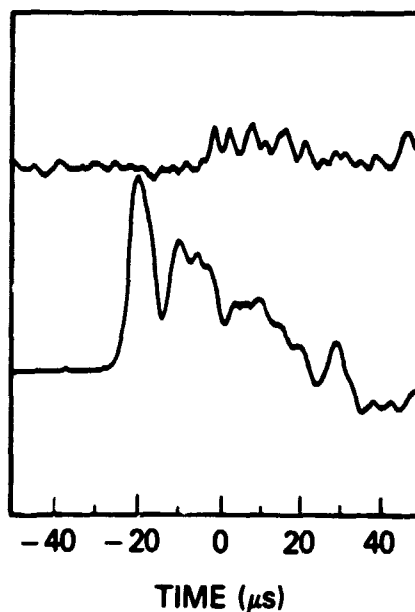on July 21, 1979 during TRIP-79.

Figure 7. Fast electric field change (bottom) and vertically
polarized radiation at 170 MHz (top) from lightning in New
Mexico. This example was recorded during TRIP-79 near
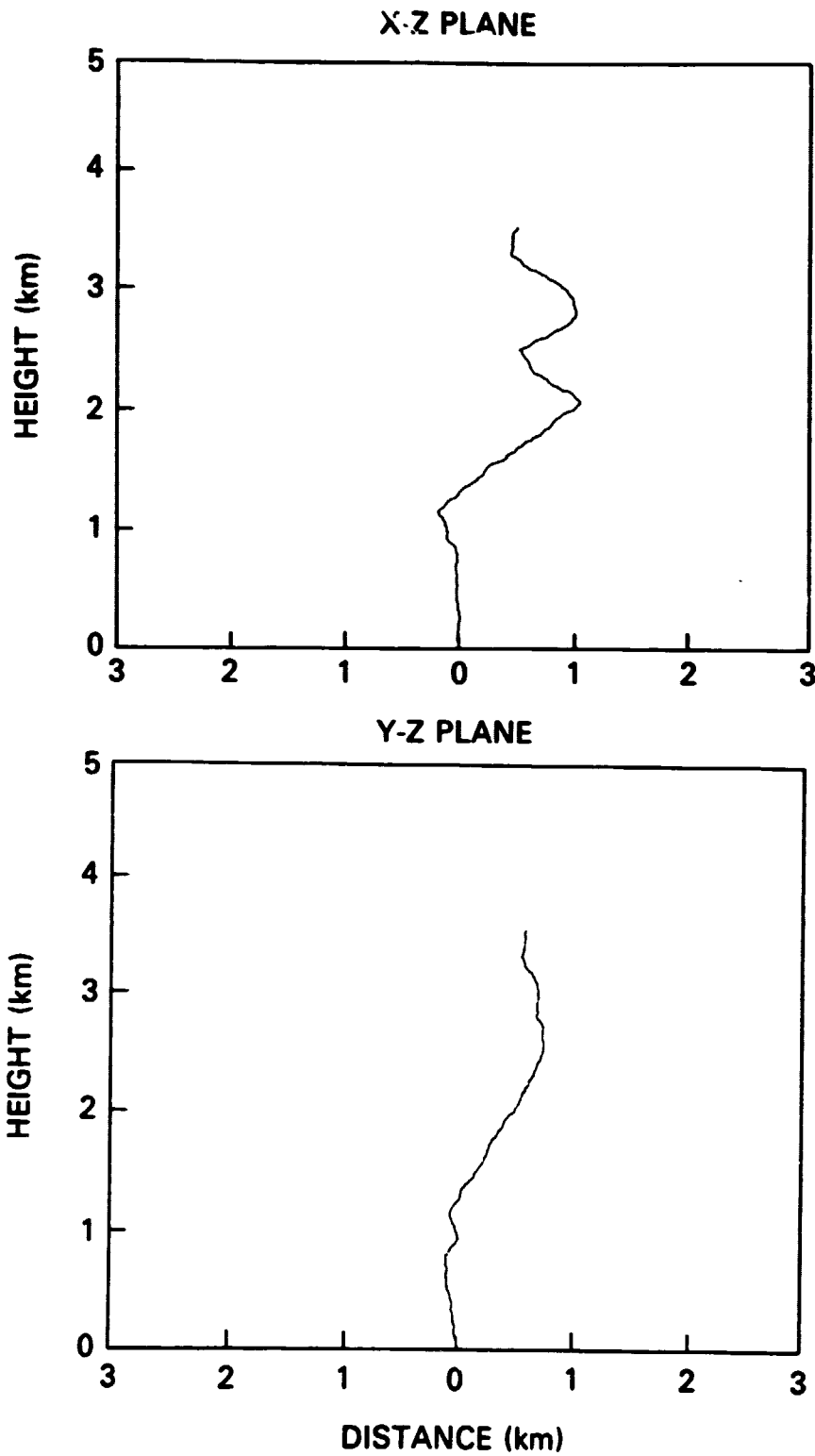Langmuir Laboratory on July 21, 1979.

26

X-Z PLANE

Y-Z PLANE

DISTANCE (km)

Figure 8. A lightning channel constructed by placing straight segments end-to-end in a random walk. There are approximately 450 segments in this example.
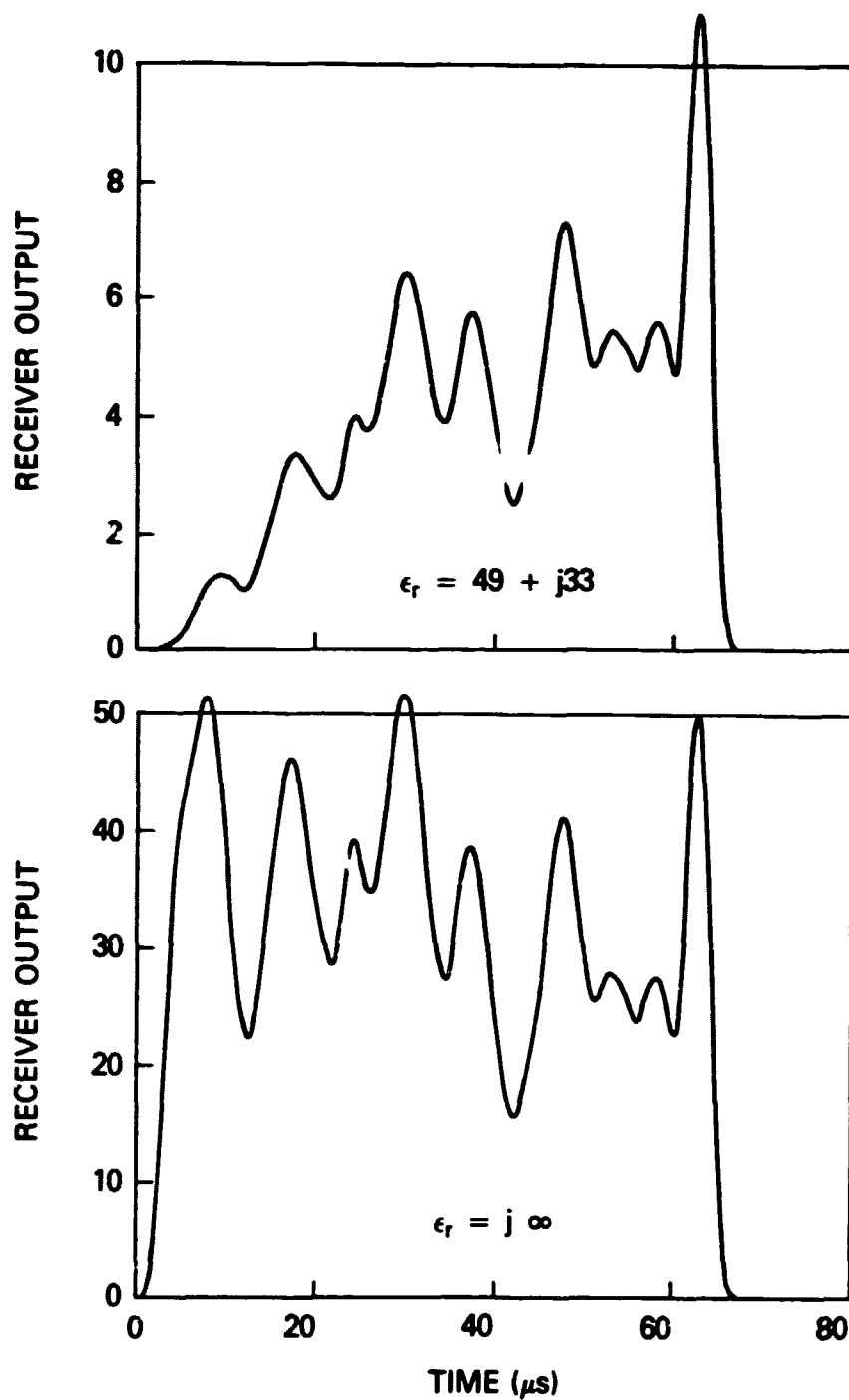
3 MHz

Figure 9. Receiver output due to radiation from the channel shown in Figure 7. The observer is 100 km from the channel on the ground. Multiply the receiver output by 6.42×10^{-5} to get $V_0(t)$ in volts.
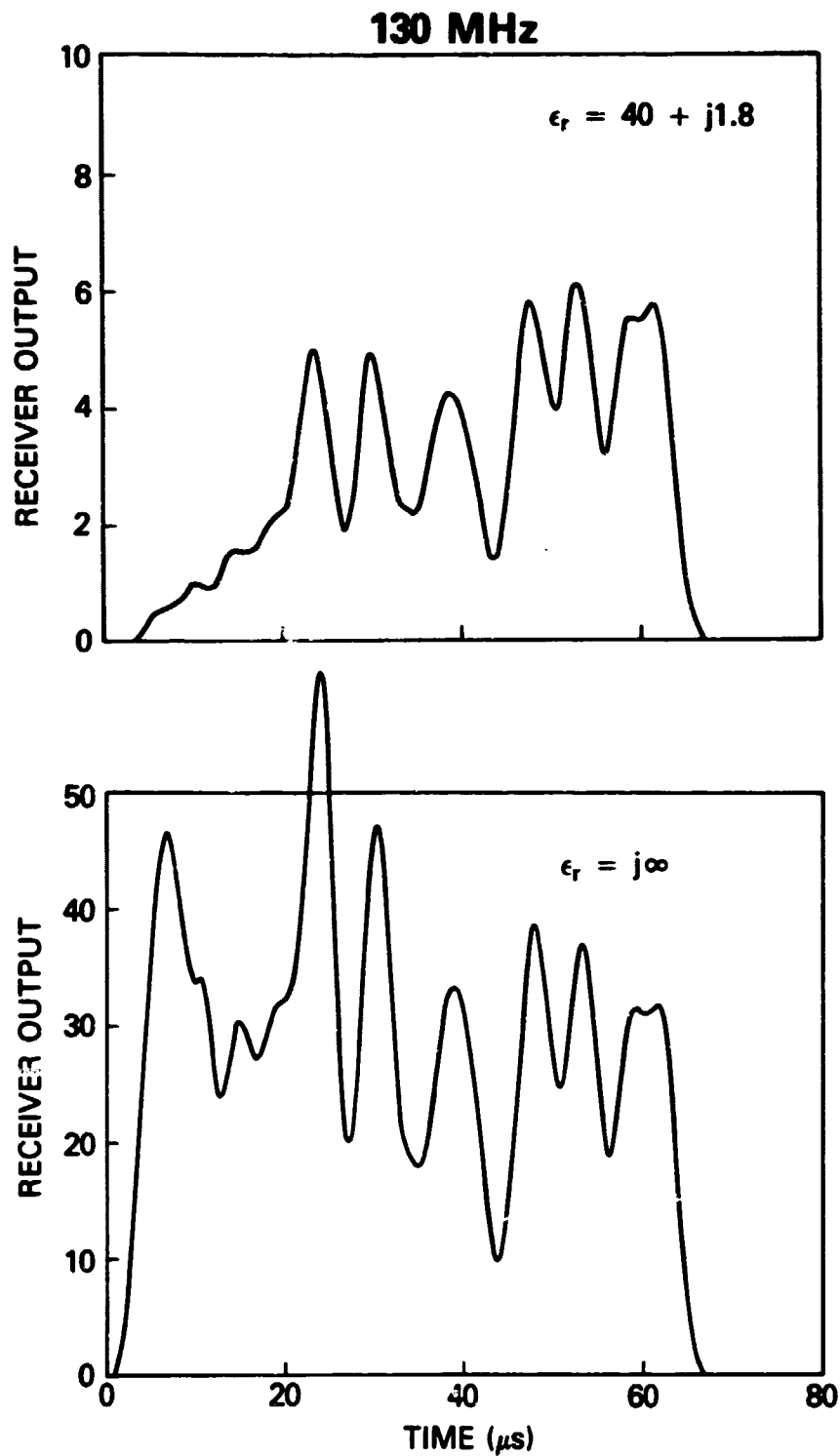
28

Figure 10. The receiver output at 130 MHz for radiation from the channel shown in Figure 7. The observer is 100 km from the channel on the ground. Multiply the receiver output by 3.42×10^{-8} to get $V_0(t)$ in volts.
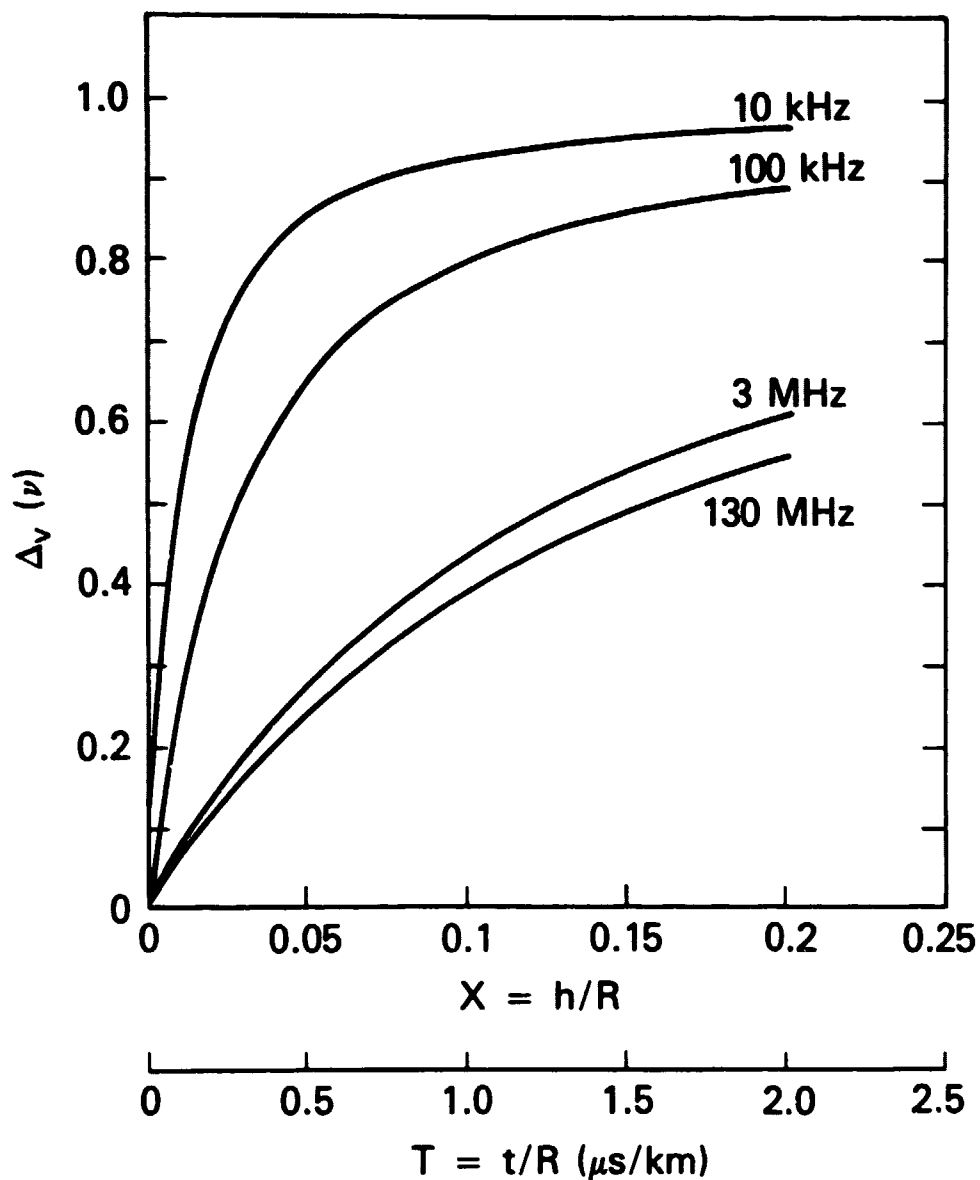
29

Figure 11. The correction factor, $\Delta_v(\nu)$ which accounts for the conductivity of the ground plane on radiation from a dipole. h is the height of the dipole and R is the distance to the observer.
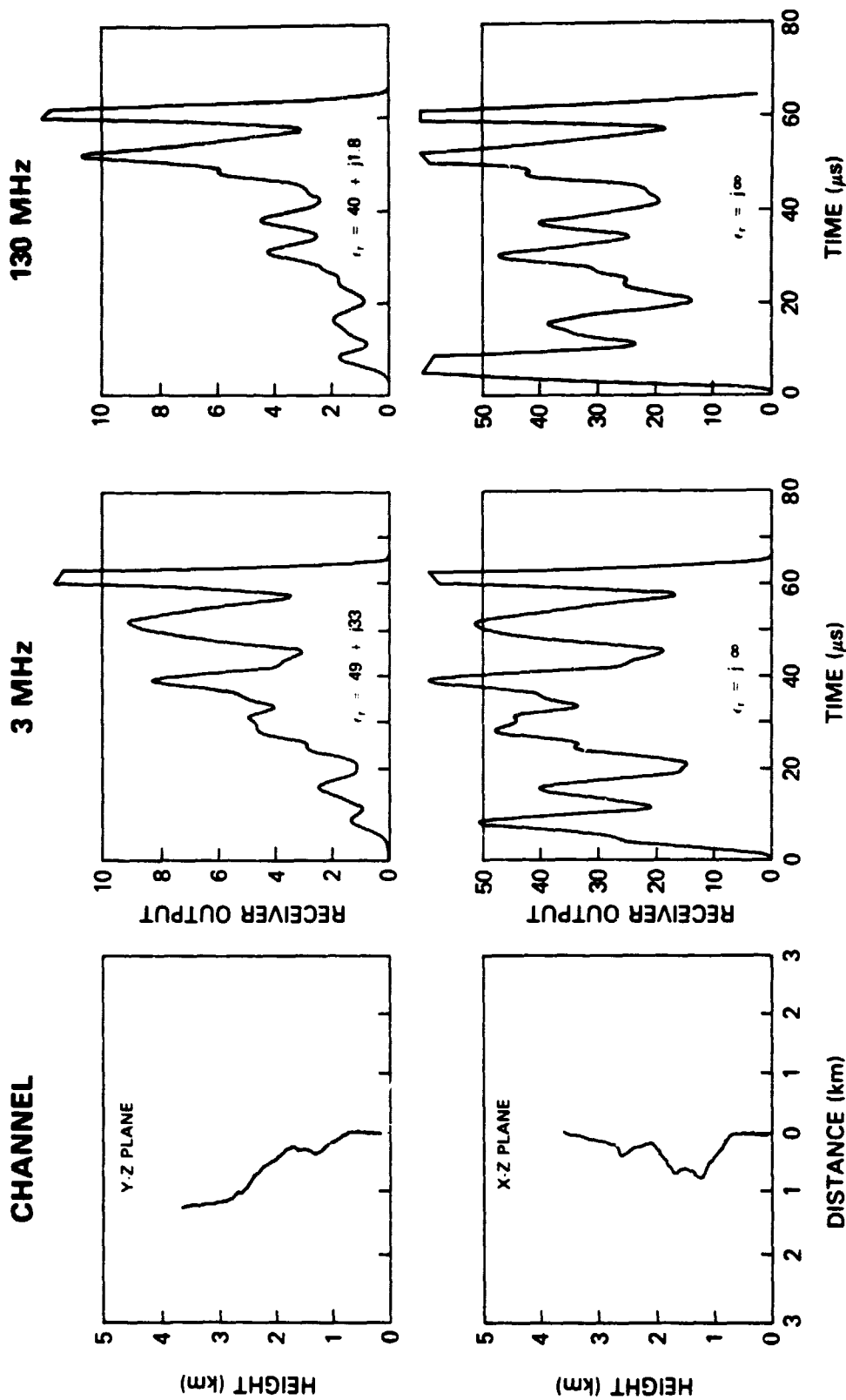
30

Figure 12. Receiver output from the channel shown to the left. The receiver output at 3 MHz and 130 MHz for an observer 100 km from the channel is shown to the right for a channel over a perfectly conducting ground plane (bottom) and finitely conducting soil (top). Multiply the receiver output by 6.42 x 10⁻⁵ at 3 MHz and 3.42 x 10⁻⁸ at 130 MHz to obtain $V_o(t)$ in volts.
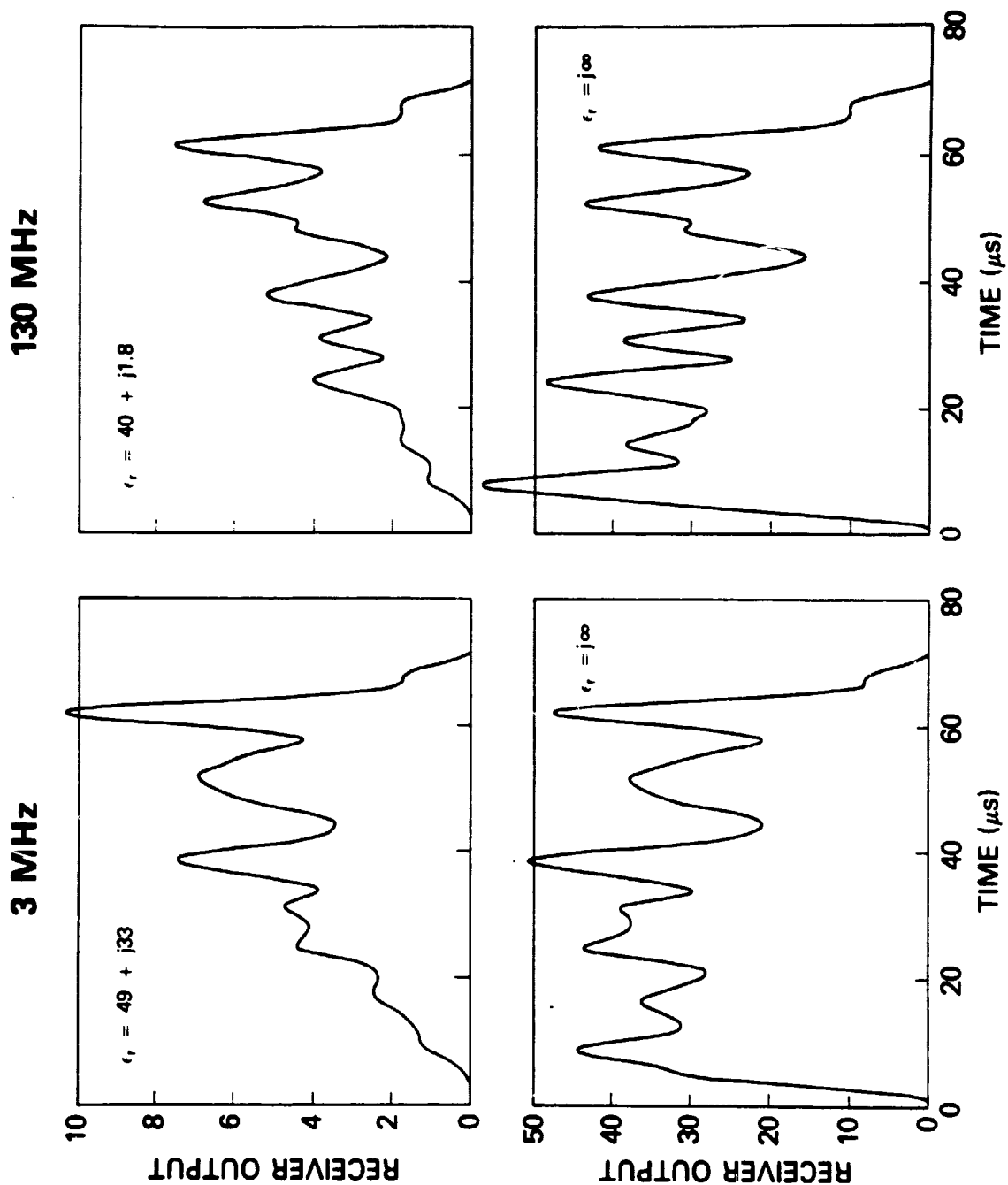
Figure 13. Average receiver output. These curves represent the average of three examples (i.e. different channels) with the observer 100 km from the channel. Multiply by 6.42 x 10⁻⁵ at 3 MHz and by 3.42 x 10⁻⁸ at 130 MHz to obtain volts.

APPENDIX A
MODEL FOR AM RADIO RECEIVER RESPONSE

It is the purpose of this appendix to derive an expression for the voltage response of an RF receiving system such as used in the experiments to measure the time delay. The RF receiving system used in these experiments consisted of an antenna, usually vertically polarized, connected to a standard AM radio receiver and followed with a post detection filter. The post detection filter was employed to reduce all measurements to a common 300 kHz bandwidth.

The antennas used were vertical dipoles or vertically polarized disk-cone antennas. These are isotropic antennas which, over the bandwidth of the measurements, can be assumed to deliver a voltage proportional to the incident vertically polarized electric field. Except for a phase which is ultimately lost in the detector, this proportionality constant is $\sqrt{\pi G/A_e}$ /k where $k = \omega\sqrt{\mu\epsilon} = 2\pi/\lambda$, G is the gain of the antenna in the horizontal plane (parallel to the ground), and A_e is the effective receiving area of the antenna (Kraus, 1966).

The AM receiver is a device for detecting and amplifying the envelope of an amplitude modulated sinusoid (carrier) at a particular frequency. This is normally done by translating the input signal to an intermediate frequency where the actual processing is done. However, the frequency translation is done for engineering purposes to make the detection more efficient, and it is not necessary to do this in order to model the receiver output. The ideal device is a perfect envelope detector in series with a filter which represents the equivalent bandwidth of the system and an ideal amplifier which represents the system gain.

For systems whose bandwidth δ is small compared to the nominal frequency, ν_0, of the measurement, these operations can be written explicitly in terms of the spectrum (Fourier transform) of the incident radiation. To do so it is convenient to write the vertical component of incident radiation, $E_z(t)$, in the form:

$$E_z(t) = 2\text{Re}\int_0^\infty E_z(\nu)e^{-j2\pi\nu t}\,d\nu \qquad (A1)$$

where Re means "real part of", where $E_z(\nu)$ is the Fourier transform of $E_z(t)$, and where the integral and factor 2 are called the complex analytic representation of $E_z(t)$ (e.g., Born and Wolf, 1959). Using this notation, the signal $V(t)$ out of the antenna and filter and into the envelope detector is:

$$V(t) = 2\text{Re}\int_0^\infty a(\nu)H(\nu)E_z(\nu)e^{-j2\pi\nu t}\,d\nu \qquad (A2)$$

where $H(\nu)$ is the Fourier transform of the filter $h(t)$ and $a(\nu) = (A/k)\sqrt{\pi G/A_e}$ is the combined effect of the antenna and an amplifier with gain, A. Although in practice the post detection filter is applied to the video output of the receiver, mathematically the effect of the post detection filter can also be included in $H(\nu)$. This will be done here and it will be assumed that the equivalent filter $H(\nu)$ has a passband centered about frequency ν_0 which is very narrow compared to ν_0. That is:

$$H(\nu) = \begin{cases} H(\nu - \nu_0) & |\nu - \nu_0| < \delta \\ 0 & |\nu - \nu_0| > \delta \end{cases} \qquad (A3)$$

and $\delta/\nu_0 \ll 1$. Using this assumption and making the change of variables $\xi = \nu - \nu_0$, Equation A2 becomes

$$V(t) = \text{Re}\left\{ e^{-j2\pi\nu_0 t}\int_{-\infty}^\infty 2a(\nu_0 + \xi)\,E_z(\nu_0 + \xi)\,H(\xi)e^{-j2\pi\xi t}\,d\xi \right\} \qquad (A4)$$

$$= |e_z(\nu_0,t)|\cos(2\pi\nu_0 t + \phi)$$

where

$$e_z(\nu_0,t) = \int_{-\infty}^\infty a(\nu_0 + \xi)\,E_z(\nu_0 + \xi)\,H(\xi)\,e^{-j2\pi\xi t}\,d\xi \qquad (A5)$$

and where the assumption that $H(\nu)$ is nonzero only in a narrow band about ν_0 (Equation A3) has been used to formally extend the lower limit of the integration in Equation A4 to $-\infty$. From Equation A4 it is clear that $V(t)$ has the form of a sinusoid, $\cos(2\pi\nu_0 t + \phi)$, at frequency ν_0, which is amplitude modulated. The output of the detector is the envelope, $|e_z(\nu_0,t)|$, of this carrier. Thus,

the output, $V_o(t)$, can be written:

$$V_o(t) = \left| \int_{-\infty}^{\infty} 2a(\nu_o + \xi)\, E_z(\nu_o + \xi)\, H(\xi) e^{-j2\pi\xi t}\, d\xi \right| \qquad (A6)$$

which is the form used in the text to compute the receiver response to an input signal, $E_z(t)$.

APPENDIX B
RADIATION FROM A CURRENT FILAMENT ABOVE A CONDUCTING EARTH

The building block used in this paper to construct a lightning channel is a straight filament on which it is assumed that current propagates at constant velocity. The purpose of this appendix is to present a solution for the radiation from such a filament which is valid when the filament is over a finitely conducting ground plane. A solution is desired for the vertically polarized components of electric field (i.e., z-component) at an observation point which is on the surface (z = 0) and far from the lightning channel compared to the height of the filament above the ground plane.

The desired solution can be constructed from the solution for radiation from a dipole (i.e., a point source) with polarization $\bar{P}$, above a conducting ground plane as illustrated in Figure B1. Radiation from the dipole is a classic problem in electromagnetic field theory originally treated by Sommerfeld (1926) and Norton (1937) and in other forms by Wait (1961) and Baños (1966). The derivation presented here is after that by Norton (1937).

Since radiation from a dipole is desired, it is convenient to solve for the fields in terms of a Hertz potential (e.g., Stratton, 1941). One obtains:

$$\bar{B} = -j\omega\mu_0\epsilon_0\epsilon_r \bar{\nabla} \times \bar{\pi} \tag{B1}$$

$$\bar{E} = k_0^2 \epsilon_r \bar{\pi} + \nabla(\bar{\nabla} \times \bar{\pi}) \tag{B2}$$

where the Hertz potential $\bar{\pi}$ is a solution to the wave equation

$$\nabla^2 \bar{\pi} + k_0^2 \epsilon_r \bar{\pi} = -\bar{P}/\epsilon_0\epsilon_r \tag{B3}$$

and $k_0 = \omega\sqrt{\mu_0\epsilon_0}$ and $\epsilon_r = \epsilon/\epsilon_0 + j\sigma/\omega\epsilon_0 = \epsilon_r' + j\epsilon_r''$. In the region above the conducting plane (z > 0) it will be assumed that $\epsilon_r = 1$.

When $\bar{P} = P_z\hat{z}$ (that is, when the dipole is vertical) only one component $\bar{\pi} = \pi_z^v\hat{z}$ is needed and one can show (e.g., Baños, 1966; Norton, 1937) that

$$\pi_z^v = \frac{jk_0P_z}{\epsilon_0} [g(\bar{r}/\bar{r}') - g(\bar{r}/\bar{r}_I') + V(\bar{r}/\bar{r}_I')] \tag{B4}$$

where

$$V(\bar{r}/\bar{r}_I') = \frac{1}{2\pi} \int_0^\infty \frac{\epsilon_r}{m + \ell\epsilon_r} \, J_0(\lambda\rho)e^{-(z'+z)\ell} \lambda \, d\lambda \qquad (B6)$$

and $\rho = \sqrt{(x'-x)^2 + (y'-y)^2}$, $\ell^2 = \lambda^2 - k_0^2$, $m^2 = \lambda^2 - k_0^2 \epsilon_r$ and where $g(\bar{r}/\bar{r}') = \exp(jk_0R)/(4\pi R)$ where $R = |\bar{r} - \bar{r}'|$ is the Green's function for the wave equation in the absence of boundaries (i.e., the free space Green's function). Also $\bar{r}_I'$ is the position the mirror image of the dipole below the ground plane and $|\bar{r} - \bar{r}_I'| = R_I$ is the distance between the observer and this image (Figure B1): $\bar{r}_I' = \bar{r}' - 2(\bar{r}' \cdot \hat{z})\hat{z}$. Using Equation B? the following form is obtained for the vertical component of electric field from the vertical dipole in the region $z > 0$:

$$E_z^v = [k_0^2 + (\partial^2/\partial z^2)]\,\pi_z^v \qquad (B6)$$

The solution when the dipole is horizontal requires two components of the Hertz potential. For example in the case of a horizontal dipole oriented along the x-axis ($\bar{P} = P_x \hat{x}$) the solution can be expressed in terms of an x- and z-component of $\bar{\pi}$: $\bar{\pi}^h = \pi_x^h \hat{x} + \pi_z^h \hat{z}$. However these components are related and the solution for E_z in this case can be written in terms of the integral $V(\bar{r}/\bar{r}_I')$, just as in the case of a vertical dipole. Following Norton (1937) one obtains:

$$E_z^h = \frac{P_x}{\epsilon_0} \cos\phi \, \frac{\partial^2}{\partial\rho\partial z} \, [V(\bar{r}/\bar{r}_I') - g(\bar{r}/\bar{r}') - g(\bar{r}/\bar{r}_I')] \qquad (B7)$$

where ρ is defined as before and $\rho \cos\phi = x - x'$. In this notation, ϕ is the conventional cylindrical coordinate measured from the x-axis. In the case of a horizontal dipole along the y-axis, the only change is that $\cos\phi$ is replaced by $\sin\phi$. For the application to the problem of the time delay in radiation from lightning, it is desired to evaluate Equation B6 and B7 when kR is large. In this case the following asymptotic approximation for $V(\bar{r}/\bar{r}')$ pertains (Norton, 1937):

$$V(\bar{r}/\bar{r}') \cong 2g(\bar{r}/\bar{r}_I') \, [1 - \xi/(1+\xi)] \qquad (B8)$$

where

B-2

$$\xi = \frac{z + z'}{R_I} \sqrt{\epsilon_r} \qquad \text{(B9)}$$

Substituting the approximation into Equation B6-7 and letting $z = 0$ (observer on the surface) one obtains

$$E_z^v = -2\omega^2 \mu_0 P_z [\xi/(1+\xi)] g(\overline{r}/\overline{r}') \qquad \text{(B10)}$$

$$E_z^h = -2\omega^2 \mu_0 [\xi/(1+\xi)] \left[1 + j \frac{R}{k_0 (z')^2 (1+\xi)} \right] (z'/R)(\overline{P}_h \cdot \nabla R) g(\overline{r}/\overline{r}') \qquad \text{(B11)}$$

where $\overline{P}_h = P_{hx} \hat{x} + P_{hy} \hat{y}$. As a check on these results, notice that in the limit $\epsilon_r \rightarrow j\infty$ one obtains:

$$E_z^v \rightarrow j\omega\mu_0(2l_v) \frac{e^{jkR}}{4\pi R} = E_{vz}^\infty \qquad \text{(B12)}$$

$$E_z^h \rightarrow j\omega\mu_0(2\overline{l}_h \cdot \nabla R)(z'/R) \frac{e^{jkR}}{4\pi R} = E_{hz}^\infty \qquad \text{(B13)}$$

where $\overline{l} = -j\omega\overline{P}$ is the current equivalent of the time varying dipole and where E_{vz}^∞ and E_{hz}^∞ are the standard results one obtains for radiation from a dipole above a perfectly conducting half-space (e.g., Jones, 1964).

Comparing B10-11 with B12-13 it is clear that one can write

$$E_z^v = \Delta_v E_{vz}^\infty \qquad \text{(B14)}$$

$$E_z^h = \Delta_h E_{hz}^\infty \qquad \text{(B15)}$$

where

$$\Delta_v = \frac{\xi}{1+\xi} \qquad \text{(B16a)}$$

$$\Delta_h = \frac{\xi}{1+\xi} \left[1 + j \frac{R}{k_0 (z')^2 (1+\xi)} \right] \qquad \text{(B16b)}$$

$$\xi = z' \sqrt{\epsilon_r} / R \qquad \text{(B16c)}$$

and z' is the height of the dipole above the surface.

It is interesting to compare the relative contributions of vertical and horizontal dipoles to E_z. Thus, from Equations B12-16 and letting $\xi \ll 1$, one obtains

$$\frac{E_z^v}{E_z^h} = \left[\frac{z'}{R} + j\frac{1}{k_o z'}\right]^{-1} \left[\frac{P_z}{\overline{P}_h \cdot \nabla R}\right] \tag{B17}$$

$$\geq \left[\frac{z'}{R} + j\frac{1}{k_o z'}\right]^{-1} \frac{P_z}{|\overline{P}_h|}$$

$$\cong (R/z')\frac{P_z}{|\overline{P}_h|} \quad \text{if } k_o z' \gg 1$$

Hence, if the dipole is several wavelengths above the surface, then for an observer far from the dipole compared to its distance above the surface ($R \gg z'$), the radiation will be much stronger from vertical dipoles than from horizontal dipoles of equal strength. In the application of the results to lightning return strokes one would expect the vertical components to be even more dominant because the channels have a predominant vertical orientation. In fact, it is a common assumption in calculating radiation from return strokes to assume that the channel is straight and vertical (e.g., Lin, Uman and Standler, 1980).

The analysis to this point has been for radiation from dipoles (i.e., infinitessimally small, point sources). The solution that is needed for the return stroke is for radiation from a filament (straight line) along which current propagates at constant velocity: That is, $\overline{I}(\nu, \overline{r}') = \hat{\ell} I(\nu) \exp(jk_o \eta \hat{\ell} \cdot \overline{r}')$ where $\hat{\ell}$ is a unit vector along the filament in the direction of propagation of the current and $\eta = c/v$ is the ratio of the speed of light in vacuum to the velocity of propagation, v, of the current pulse along the filament. In the time domain this current pulse is $I(t) = \hat{\ell} I(t - \hat{\ell} \cdot \overline{r}'/v)$. The solution for the dipole presented above is in effect a Green's function for this problem and a formal solution for the z-component of radiated electric field can be written in terms of this solution by summing along the filament. One obtains:

$$E_{(h,v)z} = \int_{filament} g_{h,v}(\overline{r}/\overline{r}') I(\nu,r') \, dr' \qquad (B18)$$

where

$$g_h(\overline{r}/\overline{r}') = j\omega\mu_0[\hat{\ell}\cdot\hat{z}] \frac{e^{jk_0R}}{2\pi R} \Delta_v \qquad (B19a)$$

$$g_v(\overline{r}/\overline{r}') = j\omega\mu_0[(\hat{\ell}\cdot \nabla R) - (\hat{\ell}\cdot\hat{z})(\hat{z}\cdot \nabla R)](z'/R) \frac{e^{jk_0R}}{2\pi R} \Delta_h \qquad (B19b)$$

$$I(\nu,\overline{r}') = I(\nu)e^{jk_0\eta \hat{\ell}\cdot\overline{r}'} \qquad (B19c)$$

In the limit $\Delta_v = \Delta_h = 1$ the Green's functions $g_{h,v}(\overline{r}/\overline{r}')$ are just the Green's functions for the z-component of electric field radiated from a current above a perfectly conducting ground plane. Denoting these Green's functions by $g_{h,v}^{\infty}(\overline{r}/\overline{r}')$ and substituting Equation B19c explicity into Equation B18, one obtains:

$$E_{(h,v)z} = \int_{filament} \Delta_{h,v} g_{h,v}^{\infty}(\overline{r}/\overline{r}') I(\nu) e^{jk_0\eta\hat{\ell}\cdot\overline{r}'} \, d\overline{r}' \qquad (B20)$$

For filaments which are sufficiently short that ξ can be assumed to be constant, the $\Delta_{h,v}$ can be taken out of the integral. After doing so, the remaining integral in Equation B20 is the conventional solution for the fields radiated to an observer on the ground from a linear travelling wave antenna above a perfectly conducting half-space. Using a fraunhofer approximation to evaluate the integral, which is valid when the observer is far from the filament compared to its length (e.g., Le Vine and Meneghini. 1978a, b), leads to Equations 4 and 5 in the text.
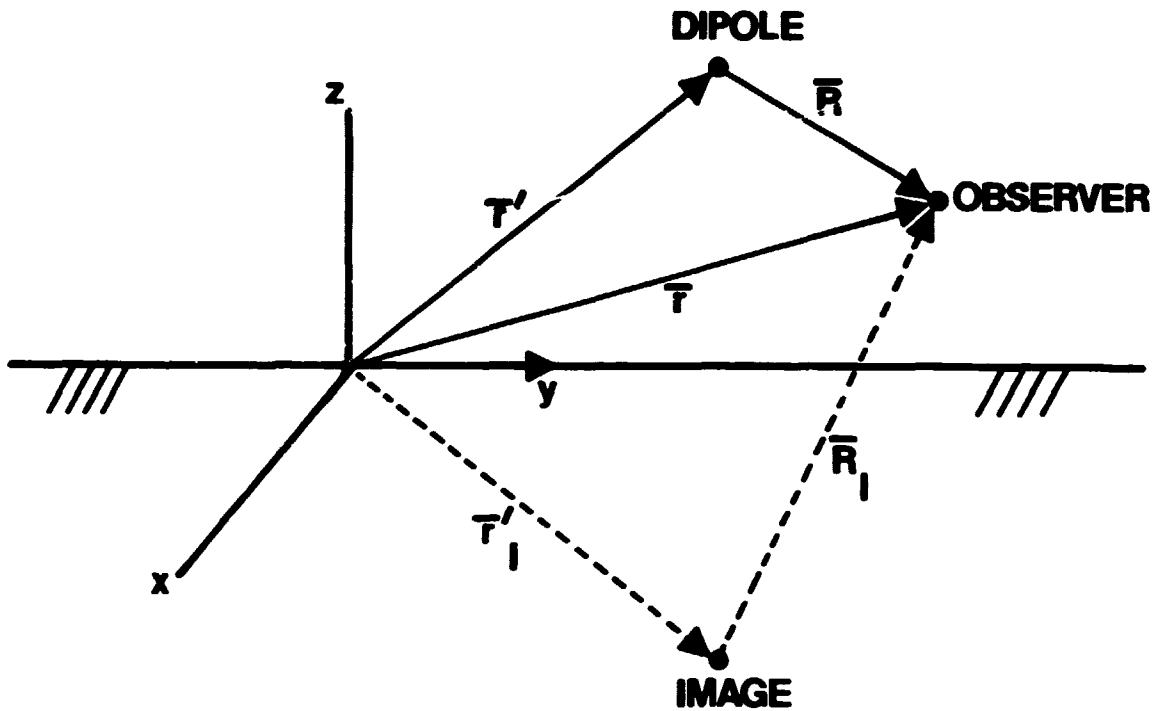
Figure B1. The geometry for calculation of radiation from a dipole over a conducting ground plane (z < 0).